HHS Public Access

Author manuscript

Cell Rep. Author manuscript; available in PMC 2016 June 16.

Published in final edited form as:

Cell Rep. 2015 June 16; 11(10): 1604–1613. doi:10.1016/j.celrep.2015.05.017.

Structural constraints determine the glycosylation of HIV-1 envelope trimers

Laura K. Pritchard[1,†], **Snezana Vasiljevic**[1,†], **Gabriel Ozorowski**[2], **Gemma E. Seabright**[1], **Albert Cupo**[3], **Rajesh Ringe**[3], **Helen J. Kim**[2], **Rogier W. Sanders**[3,4], **Katie J. Doores**[5], **Dennis R. Burton**[6,7], **Ian A. Wilson**[2], **Andrew B. Ward**[2], **John P. Moore**[3], and **Max Crispin**[1,*]

[1]Oxford Glycobiology Institute, Department of Biochemistry, University of Oxford, South Parks Road, Oxford OX1 3QU, UK [2]Department of Integrative Structural and Computational Biology, IAVI Neutralizing Antibody Center, Center for HIV/AIDS Vaccine Immunology and Immunogen Discovery, Skaggs Institute for Chemical Biology, The Scripps Research Institute, 10550 North Torrey Pines Road, La Jolla, CA 92037, USA [3]Department of Microbiology and Immunology, Weill Cornell Medical College, New York, New York, NY 10021, USA [4]Laboratory of Experimental Virology, Department of Medical Microbiology, Center for Infection and Immunity Amsterdam (CINIMA), Academic Medical Center of the University of Amsterdam, 1105 AZ Amsterdam, the Netherlands [5]King's College London School of Medicine at Guy's, King's and St Thomas' Hospitals, Guy's Hospital, Great Maze Pond, London SE1 9RT, UK [6]Department of Immunology and Microbial Science, The Scripps Research Institute, La Jolla, CA 92037, USA. International AIDS Vaccine Initiative Neutralizing Antibody Center, The Scripps Research Institute, La Jolla, CA 92037, USA. Center for HIV/AIDS Vaccine Immunology and Immunogen Discovery, The Scripps Research Institute, La Jolla, CA 92037, USA [7]Ragon Institute of Massachusetts General Hospital, Massachusetts Institute of Technology, and Harvard University, Boston, MA 02142, USA

Abstract

A highly glycosylated, trimeric envelope glycoprotein (Env) mediates HIV-1 cell entry. The high density and heterogeneity of the glycans shield Env from recognition by the immune system but, paradoxically, many potent broadly neutralizing antibodies (bNAbs) recognize epitopes involving this glycan shield. To better understand Env glycosylation and its role in bNAb recognition, we characterized a soluble, cleaved recombinant trimer (BG505 SOSIP.664) that is a close structural

* To whom correspondence should be addressed. max.crispin@bioch.ox.ac.uk.
† Co-first author

Author contributions

L.K.P., S.V., G.O., G.E.S., H.J.K. and A.C. performed experimental work. L.K.P., S.V., G.O., R.W.S., K.J.D., D.R.B., I.A.W., A.B.W., J.P.M. and M.C. analyzed data. L.K.P., G.O., K.J.D., R.W.S., D.R.B., I.A.W., A.B.W., J.P.M. and M.C. wrote the paper. J.P.M. and M.C. designed the study. All authors read and approved the final manuscript.

Competing interests

J.P.M., R.W.S., A.B.W., I.A.W. and A.C. are listed as inventors on patent applications relating to the general use of BG505 SOSIP.664 trimers and/or their production in stable CHO and 293T cell lines. The other authors have no competing interests to declare.

and antigenic mimic of native Env. Large, unprocessed oligomannose-type structures ($Man_{8-9}GlcNAc_2$) are notably prevalent on the gp120 components of the trimer, irrespective of the mammalian cell expression system or the bNAb used for affinity-purification. In contrast, gp41 subunits carry more highly processed glycans. The glycans on uncleaved, non-native oligomeric gp140 proteins are also highly processed. A homogeneous, oligomannose-dominated glycan profile is therefore a hallmark of a native Env conformation and a potential Achilles' heel that can be exploited for bNAb recognition and vaccine design.

Introduction

The HIV-1 envelope glycoprotein (Env) is a trimer of gp120-gp41 heterodimers that mediates viral entry into host cells (Liu et al., 2008). As the sole target of broadly neutralizing antibodies (bNAbs) (Hessell et al., 2009; Mascola et al., 2000; Moldt et al., 2012), it is likely that an effective prophylactic vaccine against HIV-1 will include a recombinant protein based on the Env trimer. Given that the trimer is approximately half carbohydrate by mass (Lasky et al., 1986), an important consideration for the antigenicity, and perhaps also the immunogenicity, of a recombinant version is the extent to which its glycans resemble and function like those on viral Env. The enormous relevance of glycans in HIV-1 vaccine design is underscored by the isolation of numerous distinct families of potent bNAbs whose binding is dependent upon Env glycans (Blattner et al., 2014; Falkowska et al., 2014; Garces et al., 2014; Huang et al., 2014; Kong et al., 2013; McLellan et al., 2011; Mouquet et al., 2012; Pancera et al., 2013; Pejchal et al., 2011; Scharf et al., 2014; Walker et al., 2009, 2011).

Studies on monomeric gp120 proteins have consistently identified two major subgroups of glycan structures: under-processed oligomannose and processed complex glycans (Bonomelli et al., 2011; Doores et al., 2010; Go et al., 2013; Leonard et al., 1990; Raska et al., 2010). The under-processed glycans contain multiple terminal mannose sugars (typically 5 to 9, referred to as $Man_5GlcNAc_2$ to $Man_9GlcNAc_2$). Under-processed glycans are, therefore, often referred to as "high-mannose" or "oligomannose" glycans (we prefer hereon to use the latter term). During processing in the endoplasmic reticulum (ER) and early Golgi apparatus, α-mannosidase enzymes remove a subset of mannose moieties before various other carbohydrate components are added, predominantly in the medial and late Golgi, to create complex glycans. Whether an oligomannose glycan is then further modified is not a random event; it is determined by the spatial location and accessibility of the glycan site on the folded protein. The dominant factor is most probably whether α-mannosidases can gain access to their substrates, since unprocessed glycans are sterically shielded by other glycans and/or the protein backbone. The unprocessed glycans in HIV-1 Env tend to be clustered in the "intrinsic mannose patch" (IMP), thereby creating a large exposed surface of conserved glycans that can be targeted by bNAbs and which contains multiple overlapping epitopes (Calarese et al., 2003; Garces et al., 2014; Kong et al., 2013; Mouquet et al., 2012; Murin et al., 2014; Sanders et al., 2002; Scanlan et al., 2002; Walker et al., 2009, 2011).

Glycan characterization of native, virion-derived trimers remains a challenge due to difficulties in obtaining a sample sufficient for analysis, due in large part to the very limited

numbers of Env proteins on the viral surface. Previous studies have confirmed the presence of an IMP on virion-derived gp120; however, further investigation, including characterization of gp41 glycosylation, was not possible (Bonomelli et al., 2011; Doores et al., 2010). In this study, we have investigated the glycosylation of a highly purified, recombinant, soluble Env trimer, BG505 SOSIP.664. These trimers closely mimic the structure and antigenicity of native, virion-associated Env, and their high-resolution EM and crystal structures have been determined (Julien et al., 2013; Lyumkis et al., 2013; Pancera et al., 2014; Sanders et al., 2013). We have quantified the glycan composition of BG505 SOSIP.664 trimers expressed in several cell types and purified in different ways, in comparison with other forms of recombinant Env that are being considered as candidate HIV-1 vaccines. Our results show that gp120 subunits from BG505 SOSIP.664 trimers contain a homogeneous glycan profile that is characterized by a high abundance of the largest oligomannose-type structures, $Man_{8\text{-}9}GlcNAc_2$. In contrast, glycosylation of gp41 is reflected by cell-specific processing and dominated by complex-type glycans. Analysis of uncleaved BG505 SOSIP.664 glycoproteins, as well as uncleaved gp140 oligomers from BG505 and other genotypes, revealed a much higher degree of processing, which could be correlated with more open and irregular Env configurations that, by extrapolation, reduce the structural constraints on the relevant carbohydrate processing enzymes. Thus, the quaternary structure of HIV-1 Env is, in itself, an important parameter in determining how native trimers are glycosylated.

Results

Protein-directed glycosylation of gp120 subunits of Env trimers

BG505 SOSIP.664 gp140 trimers were expressed in CHO or 293T cells and purified using a 2G12 bNAb-affinity column followed by size exclusion chromatography (SEC), as previously described (Chung et al., 2014). The CHO and 293T cell-derived trimers, purified by the same method, had similar apparent molecular weights (Figure S1). When resolved by SDS-PAGE in the presence of the reducing agent dithiothreitol (DTT), the gp120 and $gp41_{ECTO}$ domains were fully separated, indicating that the gp140 proteins had been appropriately cleaved by furin during expression (Figure S1).

The N-linked glycans were released from SDS-PAGE gel bands by protein *N*-glycosidase F (PNGase F) digestion. The gp140 band was derived from a non-reduced SDS-PAGE gel, and the gp120 and $gp41_{ECTO}$ bands from a reduced gel. Isolated glycans were fluorescently labelled with 2-aminobenzoic acid (2-AA) and analyzed by hydrophilic interaction liquid chromatography-ultra performance liquid chromatography (HILIC-UPLC) (Figure 1). The peaks in the HILIC-UPLC profiles were assigned by sequential digestion of the labelled glycans with a panel of exoglycosidases (Figure S2; Table S1). The overall profiles of the BG505 SOSIP.664 trimers from CHO and 293T cells were very similar, with both containing a large population of oligomannose glycans (Figure 1A). Integration of the chromatograms revealed that oligomannose glycans accounted for 55% and 56% of the total glycan population of the CHO and 293T-derived trimers, respectively (Table 1). $Man_8GlcNAc_2$ and $Man_9GlcNAc_2$ forms were particularly abundant, together representing 34% and 38% of the CHO and 293T-derived glycan pools, respectively.

Separation of the trimers into their constitutive subunits revealed that glycans from gp120 accounted for the majority of the overall gp140 profile, which is expected because 72 of the total 84 potential glycosylation sites on BG505 gp140 are located on the three gp120 subunits. The gp120 subunits from CHO and 293T cell-derived BG505 SOSIP.664 trimers contained 65% and 63% oligomannose glycans, respectively (Figure 1B; Table 1), with a comparable value (60%) for trimers expressed in 293F cells (Figure S3; Table S2). $Man_8GlcNAc_2$ and $Man_9GlcNAc_2$ together accounted for up to 49% of total glycan content (Table 1; Table S2; Figure S3). In contrast, oligomannose glycans were much less abundant on the $gp41_{ECTO}$ subunits (19% and 34% for CHO and 293T cell-derived trimers, respectively). The presence of a large population of complex-type glycans on the $gp41_{ECTO}$ subunits revealed the impact of the producer cell on glycosylation, with CHO cells generating more sialylated structures than 293T cells (Figure 1C; Figure S2; Table S2).

Thus, the two subunits of the trimer are processed differently, with gp120 (60-65%) having a higher oligomannose content than $gp41_{ECTO}$ (19-34%). A likely explanation is that processing enzymes face greater restrictions when accessing gp120, because the local glycan density is so much greater compared to $gp41_{ECTO}$. Analysis of a crystal structure of the BG505 SOSIP.664 trimer (Pancera et al., 2014) reveals that the 72 gp120 glycosylation sites give rise to an average density of one per ~1000 $Å^2$ surface area; for the 12 predicted gp41 glycosylation sites the corresponding value is one per ~2500 $Å^2$. Whether such differential processing and the resulting glycan composition differences are important for the function of the two subunits is not yet known.

Significantly, membrane-associated, cleaved (but non-SOSIP stabilized) BG505 EnvΔCT trimers, extracted from the cell membrane via PGT151 bNAb affinity purification (Blattner et al., 2014), were also highly enriched for oligomannose glycans and had a highly similar glycan profile to the comparable BG505 SOSIP.664 preparation (Figure S4). The similarity between the glycan content of soluble and membrane-extracted Env trimers therefore implies that the membrane does not confer additional constraints on glycan processing, and that the design and methods used to create soluble SOSIP.664 trimers do not significantly impact the resulting glycosylation.

The trimer glycan signature is independent of glycan-specific bNAb purification

Glycan-dependant bNAbs differ in their specificities for glycan structures. We therefore sought to determine whether affinity purification via a 2G12 column had affected the glycan profile of the BG505 SOSIP.664 trimers analyzed above by purifying the trimers in different ways. While 2G12 is selective for terminal Manα1→2Man on oligomannose glycans (Sanders et al., 2002; Scanlan et al., 2002), the PGT145 and PGT151 epitopes include complex glycans on the gp120 trimer apex and on $gp41_{ECTO}$, respectively (Blattner et al., 2014; Falkowska et al., 2014; McLellan et al., 2011). Moreover, PGT145 and PGT151 recognize quaternary structure-dependent epitopes that are present only on fully native trimers (Blattner et al., 2014; Falkowska et al., 2014; McLellan et al., 2011; Pugach et al., 2015). We found that trimers purified using PGT145, PGT151 and 2G12, in each case followed by SEC, had almost identical glycosylation profiles (Figure 2). The same finding was made when a His-tagged BG505 SOSIP.664 trimer was expressed in 293F cells and

affinity purified using various bNAbs (2G12, PGT151, PGT145, PG9 and b12), following Ni^{2+}-affinity chromatography and SEC (Figure S3; Table S2). Thus, irrespective of the bNAb used, the affinity-purified trimers had a very similar proportion of oligomannose glycans (60-71%). Interestingly the additional bNAb affinity purification step had little impact on the glycosylation profiles of the Ni^{2+}/SEC-purified BG505 SOSIP.664 trimers, which had a level of oligomannose glycans comparable to that observed when a bNAb affinity purification step is involved (Figure S3; Table S2).

The above findings strongly suggest that the observed dominance of large oligomannose glycoforms is an integral feature of the BG505 SOSIP.664 trimers, irrespective of the cell type used for expression (CHO, 293T, 293F). Moreover, as bNAbs with divergent glycan specificities (2G12, PGT151, PGT145, PG9) or with less glycan-dependent epitopes (b12), all recognize (i.e., purify) trimers that bear essentially indistinguishable glycan profiles, the trimer population must be highly homogeneous and consistently folded into a native conformation. Similar results from His-tag purification (i.e., glycan-independent) support this conclusion.

Uncleaved trimers undergo greater levels of glycan processing

An alternative approach to making soluble gp140 immunogens is to eliminate the cleavage site between the gp120 and $gp41_{ECTO}$ subunits (Go et al., 2014; Kovacs et al., 2012). The influence of furin cleavage on Env glycosylation is unknown. To assess whether this design difference affects glycan processing, we expressed His-tagged BG505 SOSIP.664 Env proteins without co-transfecting the furin protease. Endogenous furin is not sufficiently abundant to process all trimers transiting through the secretory pathway. Thus, both uncleaved (i.e., gp140 band) and cleaved (gp120 band) Env species were observed when SDS-PAGE was carried out under reducing conditions (Figure 3A). Comparison of the glycan composition of the gp140 and gp120 bands revealed remarkable differences; the gp140 band contained a much greater content of processed glycans than the gp120. The discrepancy was substantially greater than could be accounted for by the $gp41_{ECTO}$ subunit, which is present in the gp140 band, but not in the gp120 band (Figure 3A). When furin was co-expressed with the same His-tagged BG505 SOSIP.664 construct, all the trimers were fully cleaved (Figure 3B). The glycan profile of the resulting SDS-PAGE gp120 band was highly similar to the corresponding band derived when endogenous furin cleaved only a subset of the trimers. Thus, co-transfecting furin with SOSIP.664 trimers does not adversely affect trimer glycosylation and, in fact, emulated natural cleavage. Moreover, cleavage by furin, whether endogenous or transfected, is sufficient to create a distinct, oligomannose glycoform.

The Env quaternary structure correlates with the degree of glycan processing

To investigate why cleaved and uncleaved BG505 SOSIP.664 gp140s have such different glycan compositions, we used negative stain electron microscopy (EM) to visualize their configurations (Figure 4). The fully cleaved BG505 SOSIP.664 proteins form regular, homogeneous trimers with a characteristic propeller-like appearance (Figure 4A), which is consistent with previous studies (Chung et al., 2014). The bNAb used for affinity purification did not affect the appearance of these trimers (data not shown). For comparison,

we used the BG505 WT.SEKS gp140 protein, which has an identical sequence to the BG505 SOSIP.664 construct except that the furin cleavage site is inactivated (RRRRRR to SEKS) and the stabilizing SOSIP mutations are not included (Ringe et al., 2013). Similarly to the observations of the uncleaved BG505 SOSIP.664 sub-population (see above), the glycans on the uncleaved BG505 WT.SEKS gp140 were more highly processed than on their cleaved counterparts; oligomannose structures accounted for only 42% of the total glycan population, with $Man_8GlcNAc_2$ and $Man_9GlcNAc_2$ accounting for just 23% (Figure 4B; Table 1). When viewed by EM, the uncleaved BG505 WT.SEKS gp140 glycoproteins adopted irregular, non-native and heterogeneous configurations in which the gp120 subunits were frequently splayed out (Figure 4B). These images are in marked contrast to the closed forms of the cleaved BG505 SOSIP.664 trimers, and consistent with previous studies of several other uncleaved gp140 proteins (Ringe et al., 2013; Tran et al., 2014).

A similar correlation between quaternary structure and glycan profile was also observed when analyzing further vaccine-relevant gp140 glycoproteins from different clades. The CZA97.012 protein derives from a subtype C sequence and has been studied in multiple immunization experiments (Go et al., 2014; Kovacs et al., 2012; Nkolola et al., 2010). Like the BG505 WT.SEKS gp140, it has a knocked-out cleavage site, but also includes foldon domains near the C-termini of the $gp41_{ECTO}$ subunits to artificially drive oligomerization (Go et al., 2014; Kovacs et al., 2012; Nkolola et al., 2010). The CZA97.012 gp140 was expressed in 293T cells and purified via its C-terminal His-tag followed by SEC, as previously described (Chung et al., 2014). The glycan composition of the SEC fraction corresponding to a protein with three gp120 and three $gp41_{ECTO}$ subunits was then determined (Figure 4C). This gp140 population contained only 30% oligomannose, with just 10% of the glycans in $Man_8GlcNAc_2$ or $Man_9GlcNAc_2$ form. Once again, the EM analysis revealed that most of these gp140s adopt a splayed-open conformation with only a small fraction of particles (<10%) having a more compact appearance (Figure 4C). Similar EM results were also observed with two other uncleaved, foldon-containing glycoproteins, CN54 gp140 (clade C) and UG37 gp140 (clade A), which have also been investigated as candidate immunogens (Lewis et al., 2011, 2014; Schiffner et al., 2013). These gp140s were also predominantly irregularly shaped (Figures 4D and 4E), as described previously (Ringe et al., 2013). The observed disorder of the CN54 and UG37 gp140s again correlated with a high degree of glycan processing, the oligomannose content being 27% and 42%, respectively (Figures 4D and 4E; Table 1).

Discussion

Oligomannose glycans, which are co-translationally added to glycoproteins, are typically efficiently processed to complex structures. The presence of oligomannose-type glycans on mature, native HIV-1 Env glycoproteins represents a divergence from this default pathway of ‘self’ glycosylation and provides a potential window for immune recognition. Indeed, many potent bNAbs are glycan reactive (Blattner et al., 2014; Falkowska et al., 2014; Garces et al., 2014; Huang et al., 2014; Kong et al., 2013; McLellan et al., 2011; Mouquet et al., 2012; Pancera et al., 2013; Pejchal et al., 2011; Sanders et al., 2002; Scanlan et al., 2002; Scharf et al., 2014; Walker et al., 2009, 2011). The first-described, 2G12, binds only to the terminal Manα1→2Man moieties of oligomannose glycans (Scanlan et al., 2002), while

bNAbs such as the PGT series involve contacts with both glycans and protein (Blattner et al., 2014; Falkowska et al., 2014; Garces et al., 2014; Huang et al., 2014; Kong et al., 2013; McLellan et al., 2011; Mouquet et al., 2012; Pancera et al., 2013; Pejchal et al., 2011; Scharf et al., 2014; Walker et al., 2009, 2011). Overall, there is now widespread appreciation that vaccine candidates intended to induce bNAbs should have a glycan profile that mimics that present on native Env trimers (Bonomelli et al., 2011; Burton et al., 2012; Crispin and Bowden, 2013; Doores et al., 2010; Dunlop et al., 2010).

BG505 SOSIP.664 trimers are highly stable and homogeneous, have native-like antigenic properties, and resemble viral Env when viewed by negative stain EM (Ringe et al., 2013; Sanders et al., 2013; Yasmeen et al., 2014). Although their EM and crystal structures have been determined, it was not possible to define the processing state of the glycans from the density maps (Julien et al., 2013; Lyumkis et al., 2013; Pancera et al., 2014). Here, we found that the gp120 subunits of the same SOSIP.664 trimers have a large oligomannose content, consistent with previous reports of virion-derived Env (Bonomelli et al., 2011; Doores et al., 2010). The distribution of oligomannose glycans throughout the $Man_{5\text{-}9}GlcNAc_2$ series was particularly notable, with $Man_8GlcNAc_2$ and $Man_9GlcNAc_2$ structures accounting for up to half of the glycan population. Presumably, their existence reflects protection from α-mannosidase processing that arises through the stabilization and conformational restrictions created by a network of glycan-glycan interactions that extend across the gp120 subunits of the trimer. These structural constraints are the primary determinant of Env glycosylation, and they create a reproducible glycan profile irrespective of the producer cell. In contrast, the lack of such constraints on the $gp41_{ECTO}$ subunits results in a greater dependency on the producer cell in determining the final glycan profile. The low abundance of oligomannose structures observed on $gp41_{ECTO}$ subunits here is consistent with the previously reported resistance of virion-derived trimeric gp41 to Endo H processing (Crooks et al., 2011).

Further support for structure-driven glycan processing on the native trimer comes from analysis of uncleaved gp140 proteins. EM images of these proteins generally show three separated gp120 subunits dangling from a central $gp41_{ECTO}$ moiety to which they remain tethered by the uncleaved inter-subunit linkage (Georgiev et al., 2015; Moscoso et al., 2014; Ringe et al., 2013; Tran et al., 2014), a conclusion strongly supported by HDX-MS and surface plasmon resonance (SPR) data (Guttman et al., 2014; Ringe et al., 2013; Yasmeen et al., 2014). The EM images of uncleaved gp140s shown here are entirely consistent, with irregularly shaped forms predominating. These more open configurations are reflected in their glycosylation profiles, which display a high degree of processing; in particular, there is a markedly lower abundance of $Man_8GlcNAc_2$ and $Man_9GlcNAc_2$ structures. A prior report of the highly processed nature of the glycans on uncleaved gp140 proteins from various genotypes including CZA97.012 attributed the finding to the use of non-lymphoid cells as a production substrate for recombinant proteins (Go et al., 2014). Our results show that this is not the explanation; BG505 SOSIP.664 trimers produced in both CHO and 293T cells bear the high-oligomannose characteristic of Env trimers derived from viruses produced in lymphoid cells (Bonomelli et al., 2011; Doores et al., 2010). Instead, we show conclusively that whether the BG505 SOSIP.664 gp140 protein is furin-cleaved or not, and hence whether it does or does not adopt a native-like conformation, is the paramount factor on whether the majority of the gp120 subunit glycans remain in the oligomannose form or are

processed (Figure 5). An extension to the above findings and conclusions is that the folding and oligomerization of the furin-cleaved trimers must occur quickly enough in the Golgi apparatus to protect against significant α-mannosidase processing. Overall, the localization of furin activity and the action of Golgi α-mannosidases are critical factors that shape how the trimers are glycosylated.

The glycosylation of BG505 SOSIP.664 trimers was surprisingly homogeneous. Indeed Ni^{2+}- affinity purification of His-tagged trimers followed by SEC was sufficient to isolate a trimer population with a native-like glycosylation profile, comparable to that achieved using bNAb-affinity columns. We caution, however, that this conclusion is highly unlikely to be generalizable to all SOSIP.664 trimer preparations based on different genotypes. In particular, if non-native, misfolded trimers are present (which is not the case with BG505), they will be co-purified with properly folded trimers when a Ni^{2+}/SEC protocol is used. In contrast, a bNAb column eliminates such unwanted contaminants, particularly when a trimer-specific bNAb such as PGT145 is used (Pugach et al., 2015).

The homogeneity of BG505 SOSIP.664 trimers has implications for developing vaccine strategies aimed at inducing glycan-dependent or glycan-avoiding bNAbs (Garces et al., 2014). Previous studies have suggested that the majority of Env glycans are highly processed (Go et al., 2014; Pabst et al., 2012). The resulting complexity could be construed to constitute a barrier against the elicitation of glycan-dependent bNAbs because the target epitope is diluted. However, the predominance of oligomannose-type glycans on all BG505 SOSIP.664 glycoforms reduces or even eliminates such concerns.

In summary, native-like BG505 SOSIP.664 trimers display a glycosylation profile dominated by oligomannose-type glycans and, in particular, large $Man_8GlcNAc_2$ and $Man_9GlcNAc_2$ structures. In contrast, uncleaved gp140s lack these key properties due to their non-native structures and the resulting loss of steric constraints on glycan-processing enzymes. Do the elevated levels of oligomannose glycans on the Env trimer have some functional role, for example in viral tropism and in the infection process? While we cannot answer that question yet with any certainty, we suggest that these structures arose because HIV-1 requires a high density of Env glycans to protect underlying, vulnerable, conserved protein epitopes. Oligomannose glycans may also play a role in tropism by allowing HIV-1 to interact with cell surface lectins such as DC-SIGN (Feinberg et al., 2001; Geijtenbeek et al., 2000). Irrespective of their genesis, the oligomannose components of the glycan shield constitute an Achilles' heel on the virus that can be exploited for vaccine design.

Methods

Env trimer expression and purification

BG505 SOSIP.664 trimers were expressed in stable Flp-In™ 293T and CHO cells, and purified by 2G12-affinity chromatography (unless stated otherwise) followed by SEC to remove monomers and dimers, as described elsewhere (Chung et al., 2014). Additionally, BG505 SOSIP.664 constructs bearing a C-terminal His-tag were expressed in 293F cells as previously described (Sanders et al., 2013). Env proteins were purified from the culture supernatants by Ni^{2+}-NTA affinity columns, followed by SEC. The trimer fraction was then

used in subsequent bNAb-affinity purifications. Affinity columns were made using a CNBr-activated Sepharose 4B resin (GE Healthcare) as previously described (Sanders et al., 2013). Antibodies used to make the affinity columns were expressed in 293F cells and purified using Protein A affinity chromatography according to the manufacturer's instructions (GE Healthcare). For bnAb-affinity purification of the trimers, the binding buffer was 500 mM NaCl, 20mM Tris-HCl, pH 8, the wash buffer was 20 mM Tris-HCl, 500 mM NaCl, pH 8, and the trimers were eluted with 3M $MgCl_2$. The eluted trimers were immediately buffer-exchanged into 10 mM Tris-HCl, 75 mM NaCl, pH 8 and concentrated using a 50 kDa cutoff Vivaspin column (GE Healthcare). A His-tagged BG505 SOSIP.664 N332A mutant was generated by site-directed mutagenesis, expressed in 293F cells and purified by PGT151-affinity chromatography followed by SEC. Cleaved BG505 EnvΔCT trimers were expressed in 293F cells and purified by PGT151-affinity chromatography followed by SEC, as previously described (Blattner et al., 2014). Where the role of furin-cleavage was investigated, His-tagged BG505 SOSIP.664 was expressed in 293F cells with and without recombinant furin and the resulting glycoproteins were purified by Ni^{2+}-NTA affinity chromatography. BG505 WT.SEKS uncleaved gp140 was expressed in 293T cells and purified by 2G12-affinity chromatography followed by SEC, as previously reported (Chung et al., 2014; Ringe et al., 2013; Yasmeen et al., 2014). His-tagged, uncleaved CZA97.012 gp140 was purified by Ni^{2+}-NTA affinity chromatography followed by SEC, as previously described (Chung et al., 2014; Go et al., 2014; Kovacs et al., 2012). The uncleaved CN54 gp140 (from clade C strain 97CN001, accession number AF286226) and UG37 gp140 (from clade A strain 92/UG/037, accession number AY494974) proteins were purchased from Polymun Scientific (Vienna, Austria). These proteins are described in datasheets accessible from www.polymun.at and are purified using the anti-gp41 antibody 5F3, followed by ion-exchange chromatography.

Enzymatic release of N-linked glycans

Env trimers (10 μg), purified in various ways, were fractionated by SDS-PAGE, with and without the addition of DTT, and the gels were stained with Coomassie blue. Bands corresponding to the gp140, gp120 or $gp41_{ECTO}$ species were excised from the gels and washed alternately with acetonitrile and water, five times. N-linked glycans were then released by addition of protein *N*-glycosidase F (PNGase F) at 5000 U/ml and incubation at 37°C for 16 h, according to the manufacturer's instructions (NEB; New England Biolabs). The released glycans were subsequently eluted from gel bands by extensive washing with water, and then dried using a SpeedVac concentrator.

Fluorescent labelling of N-linked glycans

Released glycans were labelled with 2-aminobenzoic acid (2-AA) as previously described (Neville et al., 2009). Briefly, glycans were resuspended in 30 μl of water followed by addition of 80 μl of labelling mixture (30 mg/ml 2-AA and 45 mg/ml sodium cyanoborohydride in a solution of sodium acetate trihydrate [4% w/v] and boric acid [2% w/v] in methanol). Samples were then incubated at 80°C for 1 h. Excess label was removed using Spe-ed Amide-2 cartridges, as previously described (Neville et al., 2009).

Hydrophilic interaction liquid chromatography-ultra performance liquid chromatography

Fluorescently labelled glycans were resolved by hydrophilic interaction liquid chromatography-ultra performance liquid chromatography (HILIC-UPLC) using a 2.1 mm × 10 mm Acquity BEH Amide Column (1.7 m particle size) (Waters, Elstree, UK). The following gradient was run: time = 0 min (*t* = 0): 22.0% A, 78.0% B (flow rate of 0.5 ml/min); *t* = 38.5: 44.1% A, 55.9% B (0.5 ml/min); *t* = 39.5: 100% A, 0% B (0.25 ml/min); *t* = 44.5: 100% A, 0% B (0.25 ml/min); *t* = 46.5: 22.0% A, 78.0% B (0.5 ml/min), *t* = 48: 22.0% A, 78.0% B (0.5 ml/min), where solvent A was 50 mM ammonium formate, pH 4.4, and solvent B was acetonitrile. Fluorescence was measured using an excitation wavelength of 250 nm and a detection wavelength of 428 nm. Data processing was performed using Empower 3 software. The percentage abundance of oligomannose-type glycans was calculated by integration of the relevant peak areas before and after Endo H digestion, following normalization.

Exoglycosidase sequencing of N-linked glycans

The structures of N-linked glycans were determined by sequential digestion of labelled glycans with a panel of exoglycosidases. The enzymes used were: neuraminidase from *Clostridium perfringens* (NEB), α-L-fucosidase from bovine kidney (Sigma), β1,4-galactosidase from *Streptococcus pneumoniae*, β-*N*-acetylglucosaminidase from *S. pneumonia* and α(1-2,3,6)-mannosidase from Jack bean (QA Bio). Endoglycosidase H (NEB) was used for quantitation of oligomannose structures. Digestions were performed at 37°C for 16 h, according to manufacturers' instructions. The digested glycans were purified using a PVDF protein-binding membrane plate (Millipore) prior to HILIC-UPLC analysis.

Negative stain electron microscopy

Env proteins were prepared for negative stain electron microscopy (EM) analysis as previously described (Pugach et al., 2015; Ringe et al., 2013; Sanders et al., 2013). Briefly, a 3 μL aliquot containing ~0.03 mg/mL of Env protein was applied for 5 s onto a carbon-coated 400 Cu mesh grid that had been glow discharged at 20 mA for 30 s, then negatively stained with 2% (w/v) uranyl formate for 60 s. Data were collected using an FEI Tecnai T12 electron microscope operating at 120 keV, with an electron dose of ~25 e-/Å^2 and a magnification of 52,000× that resulted in a pixel size of 2.05 Å at the specimen plane. Images were acquired with a Tietz TemCam-F416 CMOS camera using a nominal defocus range of 1000 nm.

Data processing methods were adapted from those used previously (Pugach et al., 2015; Ringe et al., 2013; Sanders et al., 2013). In summary, the Appion software package (Voss et al., 2009) was used to automatically pick particles, create stacks, and calculate reference-free, two-dimensional (2D) class averages with iterative MSA/MRA (Ogura et al., 2003). The 2D class averages were visually inspected and the classes were segregated into one of three structural groups labelled "closed", "open" or "non-native" as described previously (Pugach et al., 2015). The amount of native-like particles was defined as the sum of "closed" and "open" particles.

Supplementary Material

Refer to Web version on PubMed Central for supplementary material.

Acknowledgements

We would like to dedicate this article in memory of our good friend and greatly admired colleague, Dr. Chris Scanlan. The CN54 gp140 and UG37 gp140 proteins were kindly provided by Professor Quentin Sattentau (University of Oxford). We thank Prof. Raymond A. Dwek FRS for constant unwavering support and insightful discussions. L.K.P. has been supported by a Scholarship from the Department of Biochemistry, University of Oxford. M.C. is a Fellow of Oriel College, Oxford. This work was supported by NIH HIVRAD grant P01 AI082362, International AIDS Vaccine Initiative Neutralizing Antibody Center CAVD grant (Glycan characterization and Outer Domain glycoform design), the Scripps CHAVI-ID (1UM1AI100663), and the Medical Research Council MR/K024426/1. R.W.S. is a recipient of a Vidi grant from the Netherlands Organization for Scientific Research (NWO) and a Starting Investigator Grant from the European Research Council (ERC-StG-2011–280829-SHEV).

Abbreviations

2-AA	2-aminobenzoic acid
bNAb	broadly neutralizing antibody
CHO	Chinese Hamster Ovary
DTT	dithiothreitol
Env	Envelope glycoprotein
EM	electron microscopy
Fuc	Fucose
Gal	Galactose
GlcNAc	*N*-acetylglucosamine
HDX-MS	hydrogen deuterium exchange-mass spectrometry
HILIC-UPLC	hydrophilic interaction liquid chromatography -ultra performance liquid chromatography
HIV-1	human immunodeficiency virus type 1
IMP	intrinsic mannose patch
Man	Mannose
Neu5Ac	*N*-acetylneuraminic acid
PNGase F	protein *N*-glycosidase F
SDS-PAGE	sodium dodecyl sulphate-polyacrylamide gel electrophoresis
SEC	size exclusion chromatography
SPR	surface plasmon resonance

References

Blattner C, Lee JH, Sliepen K, Derking R, Falkowska E, de la Peña AT, Cupo A, Julien J-P, van Gils M, Lee PS, et al. Structural delineation of a quaternary, cleavage-dependent epitope at the gp41-gp120 interface on intact HIV-1 Env trimers. Immunity. 2014; 40:669–680.

Bonomelli C, Doores KJ, Dunlop DC, Thaney V, Dwek R. a, Burton DR, Crispin M, Scanlan CN. The glycan shield of HIV is predominantly oligomannose independently of production system or viral clade. PLoS One. 2011; 6:e23521. [PubMed: 21858152]

Burton DR, Ahmed R, Barouch DH, Butera ST, Crotty S, Godzik A, Kaufmann DE, McElrath MJ, Nussenzweig MC, Pulendran B, et al. A blueprint for HIV vaccine discovery. Cell Host Microbe. 2012; 12:396–407. [PubMed: 23084910]

Calarese, D. a; Scanlan, CN.; Zwick, MB.; Deechongkit, S.; Mimura, Y.; Kunert, R.; Zhu, P.; Wormald, MR.; Stanfield, RL.; Roux, KH., et al. Antibody domain exchange is an immunological solution to carbohydrate cluster recognition. Science. 2003; 300:2065–2071. [PubMed: 12829775]

Chung NP, Matthews K, Kim HJ, Ketas TJ, Golabek M, de Los Reyes K, Korzun J, Yasmeen A, Sanders RW, Klasse PJ, et al. Stable 293 T and CHO cell lines expressing cleaved, stable HIV-1 envelope glycoprotein trimers for structural and vaccine studies. Retrovirology. 2014; 11:33. [PubMed: 24767177]

Crispin M, Bowden TA. Antibodies expose multiple weaknesses in the glycan shield of HIV. Nat. Struct. Mol. Biol. 2013; 20:771–772. [PubMed: 23984441]

Crooks ET, Tong T, Osawa K, Binley JM. Enzyme digests eliminate nonfunctional Env from HIV-1 particle surfaces, leaving native Env trimers intact and viral infectivity unaffected. J. Virol. 2011; 85:5825–5839. [PubMed: 21471242]

Doores KJ, Bonomelli C, Harvey DJ, Vasiljevic S, Dwek RA, Burton DR. Envelope glycans of immunodeficiency virions are almost entirely oligomannose antigens. Proc. Natl. Acad. Sci. U. S. A. 2010; 107:13800–13805. [PubMed: 20643940]

Dunlop DC, Bonomelli C, Mansab F, Vasiljevic S, Doores KJ, Wormald MR, Palma AS, Feizi T, Harvey DJ, Dwek R, et al. Polysaccharide mimicry of the epitope of the broadly neutralizing anti-HIV antibody, 2G12, induces enhanced antibody responses to self oligomannose glycans. Glycobiology. 2010; 20:812–823. [PubMed: 20181792]

Falkowska E, Le KM, Ramos A, Doores KJ, Lee JH, Blattner C, Ramirez A, Derking R, van Gils MJ, Liang C-H, et al. Broadly neutralizing HIV antibodies define a glycan-dependent epitope on the prefusion conformation of gp41 on cleaved envelope trimers. Immunity. 2014; 40:657–668. [PubMed: 24768347]

Feinberg H, Mitchell D. a, Drickamer K, Weis WI. Structural basis for selective recognition of oligosaccharides by DC-SIGN and DC-SIGNR. Science (80−.). 2001; 294:2163–2166.

Garces F, Sok D, Kong L, McBride R, Kim HJ, Saye-Francisco KF, Julien J-P, Hua Y, Cupo A, Moore JP, et al. Structural evolution of glycan recognition by a family of potent HIV antibodies. Cell. 2014; 159:69–79. [PubMed: 25259921]

Geijtenbeek TB, Torensma R, van Vliet SJ, van Duijnhoven GC, Adema GJ, van Kooyk Y, Figdor CG. Identification of DC-SIGN, a novel dendritic cell-specific ICAM-3 receptor that supports primary immune responses. Cell. 2000; 100:575–585. [PubMed: 10721994]

Georgiev IS, Joyce MG, Yang Y, Sastry M, Zhang B, Baxa U, Chen RE, Druz A, Lees CR, Narpala S, et al. Single-chain soluble BG505.SOSIP gp140 trimers as structural and antigenic mimics of mature closed HIV-1 Env. J. Virol. Epub ahead. 2015

Go EP, Liao H-X, Alam SM, Hua D, Haynes BF, Desaire H. Characterization of host-cell line specific glycosylation profiles of early transmitted/founder HIV-1 gp120 envelope proteins. J. Proteome Res. 2013; 12:1223–1234. [PubMed: 23339644]

Go EP, Hua D, Desaire H. Glycosylation and disulfide bond analysis of transiently and stably expressed clade C HIV-1 gp140 trimers in 293T cells identifies disulfide heterogeneity present in both proteins and differences in O-linked glycosylation. J. Proteome Res. 2014; 13:4012–4027. [PubMed: 25026075]

Guttman M, Garcia NK, Cupo A, Matsui T, Julien J-P, Sanders RW, Wilson I. a, Moore JP, Lee KK. CD4-induced activation in a soluble HIV-1 Env trimer. Structure. 2014; 22:974–984. [PubMed: 24931470]

Hessell AJ, Rakasz EG, Poignard P, Hangartner L, Landucci G, Forthal DN, Koff WC, Watkins DI, Burton DR. Broadly neutralizing human anti-HIV antibody 2G12 is effective in protection against mucosal SHIV challenge even at low serum neutralizing titers. PLoS Pathog. 2009; 5:e1000433. [PubMed: 19436712]

Huang J, Kang BH, Pancera M, Lee JH, Tong T, Feng Y, Georgiev IS, Chuang G-Y, Druz A, Doria-Rose N. a. et al. Broad and potent HIV-1 neutralization by a human antibody that binds the gp41–gp120 interface. Nature. 2014; 515:138–142. [PubMed: 25186731]

Julien J-P, Cupo A, Sok D, Stanfield RL, Lyumkis D, Deller MC, Klasse P-J, Burton DR, Sanders RW, Moore JP, et al. Crystal structure of a soluble cleaved HIV-1 envelope trimer. Science. 2013; 342:1477–1483. [PubMed: 24179159]

Kong L, Lee JH, Doores KJ, Murin CD, Julien J, Mcbride R, Liu Y, Marozsan A, Cupo A, Klasse P, et al. Supersite of immune vulnerability on the glycosylated face of HIV-1 envelope glycoprotein gp120. Nat. Struct. Mol. Biol. Mol. Biol. 2013; 20:796–803.

Kovacs JM, Nkolola JP, Peng H, Cheung A, Perry J, Miller C. a, Seaman MS, Barouch DH, Chen B. HIV-1 envelope trimer elicits more potent neutralizing antibody responses than monomeric gp120. Proc. Natl. Acad. Sci. U. S. A. 2012; 109:12111–12116. [PubMed: 22773820]

Lasky L, Groopman J, Fennie C, Benz P, Capon D, Dowbenko D, Nakamura G, Nunes W, Renz M, Berman P. Neutralization of the AIDS retrovirus by antibodies to a recombinant envelope glycoprotein. Science. 1986; 233:209–212. [PubMed: 3014647]

Leonard CK, Spellman MW, Riddle L, Harris RJ, Thomas JN, Gregory TJ. Assignment of intrachain disulfide bonds and characterization of potential glycosylation sites of the type 1 recombinant human immunodeficiency virus envelope glycoprotein (gp120) expressed in Chinese hamster ovary cells. J. Biol. Chem. 1990; 265:10373–10382. [PubMed: 2355006]

Lewis DJ, Fraser C. a, Mahmoud AN, Wiggins RC, Woodrow M, Cope A, Cai C, Giemza R, Jeffs S. a, Manoussaka M, et al. Phase I randomised clinical trial of an HIV-1(CN54), clade C, trimeric envelope vaccine candidate delivered vaginally. PLoS One. 2011; 6:e25165. [PubMed: 21984924]

Lewis DJM, Wang Y, Huo Z, Giemza R, Babaahmady K, Rahman D, Shattock RJ, Singh M, Lehner T. Effect of vaginal immunization with HIVgp140 and HSP70 on HIV-1 replication and innate and T cell adaptive immunity in women. J. Virol. 2014; 88:11648–11657. [PubMed: 25008917]

Liu J, Bartesaghi A, Borgnia MJ, Sapiro G, Subramaniam S. Molecular architecture of native HIV-1 gp120 trimers. Nature. 2008; 455:109–113. [PubMed: 18668044]

Lyumkis D, Julien J-P, de Val N, Cupo A, Potter CS, Klasse P-J, Burton DR, Sanders RW, Moore JP, Carragher B, et al. Cryo-EM structure of a fully glycosylated soluble cleaved HIV-1 envelope trimer. Science. 2013; 342:1484–1490. [PubMed: 24179160]

Mascola JR, Stiegler G, VanCott TC, Katinger H, Carpenter CB, Hanson CE, Beary H, Hayes D, Frankel SS, Birx DL, et al. Protection of macaques against vaginal transmission of a pathogenic HIV-1/SIV chimeric virus by passive infusion of neutralizing antibodies. Nat. Med. 2000; 6:207–210. [PubMed: 10655111]

McLellan JS, Pancera M, Carrico C, Gorman J, Julien J-P, Khayat R, Louder R, Pejchal R, Sastry M, Dai K, et al. Structure of HIV-1 gp120 V1/V2 domain with broadly neutralizing antibody PG9. Nature. 2011; 480:336–343. [PubMed: 22113616]

Moldt B, Rakasz EG, Schultz N, Chan-Hui P-Y, Swiderek K, Weisgrau KL, Piaskowski SM, Bergman Z, Watkins DI, Poignard P, et al. Highly potent HIV-specific antibody neutralization in vitro translates into effective protection against mucosal SHIV challenge in vivo. Proc. Natl. Acad. Sci. U. S. A. 2012; 109:18921–18925. [PubMed: 23100539]

Moscoso CG, Xing L, Hui J, Hu J, Kalkhoran MB, Yenigun OM, Sun Y, Paavolainen L, Martin L, Vahlne A, et al. Trimeric HIV Env provides epitope occlusion mediated by hypervariable loops. Sci. Rep. 2014; 4:7025. [PubMed: 25395053]

Mouquet H, Scharf L, Euler Z, Liu Y, Eden C, Scheid JF, Halper-Stromberg A, Gnanapragasam PNP, Spencer DIR, Seaman MS, et al. Complex-type N-glycan recognition by potent broadly

neutralizing HIV antibodies. Proc. Natl. Acad. Sci. U. S. A. 2012; 109:E3268–E3277. [PubMed: 23115339]

Murin CD, Julien J-P, Sok D, Stanfield RL, Khayat R, Cupo A, Moore JP, Burton DR, Wilson IA, Ward AB. Structure of 2G12 Fab2 in complex with soluble and fully glycosylated HIV-1 Env by negative-stain single particle electron microscopy. J. Virol. 2014; 88:10177–10188. [PubMed: 24965454]

Neville DCA, Dwek RA, Butters TD. Development of a single column method for the separation of lipid- and protein-derived oligosaccharides. J. Proteome Res. 2009; 8:681–687. [PubMed: 19099509]

Nkolola JP, Peng H, Settembre EC, Freeman M, Grandpre LE, Devoy C, Lynch DM, La Porte A, Simmons NL, Bradley R, et al. Breadth of neutralizing antibodies elicited by stable, homogeneous clade A and clade C HIV-1 gp140 envelope trimers in guinea pigs. J. Virol. 2010; 84:3270–3279. [PubMed: 20053749]

Ogura T, Iwasaki K, Sato C. Topology representing network enables highly accurate classification of protein images taken by cryo electron-microscope without masking. J. Struct. Biol. 2003; 143:185–200.

Pabst M, Chang M, Stadlmann J, Altmann F. Glycan profiles of the 27 N-glycosylation sites of the HIV envelope protein CN54gp140. Biol. Chem. 2012; 393:719–730. [PubMed: 22944675]

Pancera M, Shahzad-Ul-Hussan S, Doria-Rose N. a, McLellan JS, Bailer RT, Dai K, Loesgen S, Louder MK, Staupe RP, Yang Y, et al. Structural basis for diverse N-glycan recognition by HIV-1-neutralizing V1-V2-directed antibody PG16. Nat. Struct. Mol. Biol. 2013; 20:804–813. [PubMed: 23708607]

Pancera M, Zhou T, Druz A, Georgiev IS, Soto C, Gorman J, Huang J, Acharya P, Chuang G-Y, Ofek G, et al. Structure and immune recognition of trimeric pre-fusion HIV-1 Env. Nature. 2014; 514:455–461. [PubMed: 25296255]

Pejchal R, Doores KJ, Walker LM, Khayat R, Huang P-S, Wang S-K, Stanfield RL, Julien J-P, Ramos A, Crispin M, et al. A potent and broad neutralizing antibody recognizes and penetrates the HIV glycan shield. Science. 2011; 334:1097–1103. [PubMed: 21998254]

Pugach P, Ozorowski G, Cupo A, Ringe R, Yasmeen A, de Val N, Derking R, Kim HJ, Korzun J, Golabek M, et al. A native-like SOSIP.664 trimer based on an HIV-1 subtype B env gene. J. Virol. 2015; 89:3380–3395. [PubMed: 25589637]

Raska M, Takahashi K, Czernekova L, Zachova K, Hall S, Moldoveanu Z, Elliott MC, Wilson L, Brown R, Jancova D, et al. Glycosylation patterns of HIV-1 gp120 depend on the type of expressing cells and affect antibody recognition. J. Biol. Chem. 2010; 285:20860–20869. [PubMed: 20439465]

Ringe RP, Sanders RW, Yasmeen A, Kim HJ, Hyun J, Cupo A, Korzun J. Cleavage strongly influences whether soluble HIV-1 envelope glycoprotein trimers adopt a native-like conformation. Proc. Natl. Acad. Sci. U. S. A. 2013; 110:18256–18261. [PubMed: 24145402]

Sanders RW, Venturi M, Schiffner L, Kalyanaraman R, Katinger H, Lloyd KO, Kwong PD, Moore JP. The mannose-dependent epitope for neutralizing antibody 2G12 on human immunodeficiency virus type 1 glycoprotein gp120. J. Virol. 2002; 76:7293–7305. [PubMed: 12072528]

Sanders RW, Derking R, Cupo A, Julien J-P, Yasmeen A, de Val N, Kim HJ, Blattner C, de la Peña AT, Korzun J, et al. A next-generation cleaved, soluble HIV-1 Env trimer, BG505 SOSIP.664 gp140, expresses multiple epitopes for broadly neutralizing but not non-neutralizing antibodies. PLoS Pathog. 2013; 9:e1003618.

Scanlan CN, Pantophlet R, Wormald MR, Saphire EO, Stanfield R, Wilson IA, Katinger H, Dwek RA, Rudd PM, Burton DR. The broadly neutralizing anti-human immunodeficiency virus type 1 antibody 2G12 recognizes a cluster of α1→2 mannose residues on the outer face of gp120. J. Virol. 2002; 76:7306–7321. [PubMed: 12072529]

Scharf L, Scheid JF, Lee JH, West AP, Chen C, Gao H, Gnanapragasam PNP, Mares R, Seaman MS, Ward AB, et al. Antibody 8ANC195 reveals a site of broad vulnerability on the HIV-1 envelope spike. Cell Rep. 2014; 7:785–795. [PubMed: 24767986]

Schiffner T, Kong L, Duncan C.J. a, Back JW, Benschop JJ, Shen X, Huang PS, Stewart-Jones GB, DeStefano J, Seaman MS, et al. Immune focusing and enhanced neutralization induced by HIV-1 gp140 chemical cross-linking. J. Virol. 2013; 87:10163–10172. [PubMed: 23843636]

Tran K, Poulsen C, Guenaga J, de Val N, Wilson R, Sundling C, Li Y, Stanfield RL, Wilson IA, Ward AB, et al. Vaccine-elicited primate antibodies use a distinct approach to the HIV-1 primary receptor binding site informing vaccine design. Proc. Natl. Acad. Sci. 2014; 111:E738–E747.

Voss NR, Yoshioka CK, Radermacher M, Potter CS, Carragher B. DoG Picker and TiltPicker: software tools to facilitate particle selection in single particle electron microscopy. J. Struct. Biol. 2009; 166:205–213.

Walker LM, Phogat SK, Chan-Hui P-Y, Wagner D, Phung P, Goss JL, Wrin T, Simek MD, Fling S, Mitcham JL, et al. Broad and potent neutralizing antibodies from an African donor reveal a new HIV-1 vaccine target. Science. 2009; 326:285–289. [PubMed: 19729618]

Walker LM, Huber M, Doores KJ, Falkowska E, Pejchal R, Julien J-P, Wang S-K, Ramos A, Chan-Hui P-Y, Moyle M, et al. Broad neutralization coverage of HIV by multiple highly potent antibodies. Nature. 2011; 477:466–470. [PubMed: 21849977]

Yasmeen A, Ringe R, Derking R, Cupo A, Julien J-P, Burton DR, Ward AB, Wilson I. a, Sanders RW, Moore JP, et al. Differential binding of neutralizing and non-neutralizing antibodies to native-like soluble HIV-1 Env trimers, uncleaved Env proteins, and monomeric subunits. Retrovirology. 2014; 11:41. [PubMed: 24884783]

Highlights

- Native-like, cleaved HIV-1 Env mimetics are dominated by under-processed *N*-glycans.
- In contrast, non-native uncleaved trimers undergo greater glycan processing.
- The Env quaternary structure dictates the degree of glycan processing that can occur.
- The abundance of homogeneous oligomannose glycans is promising for vaccine design.

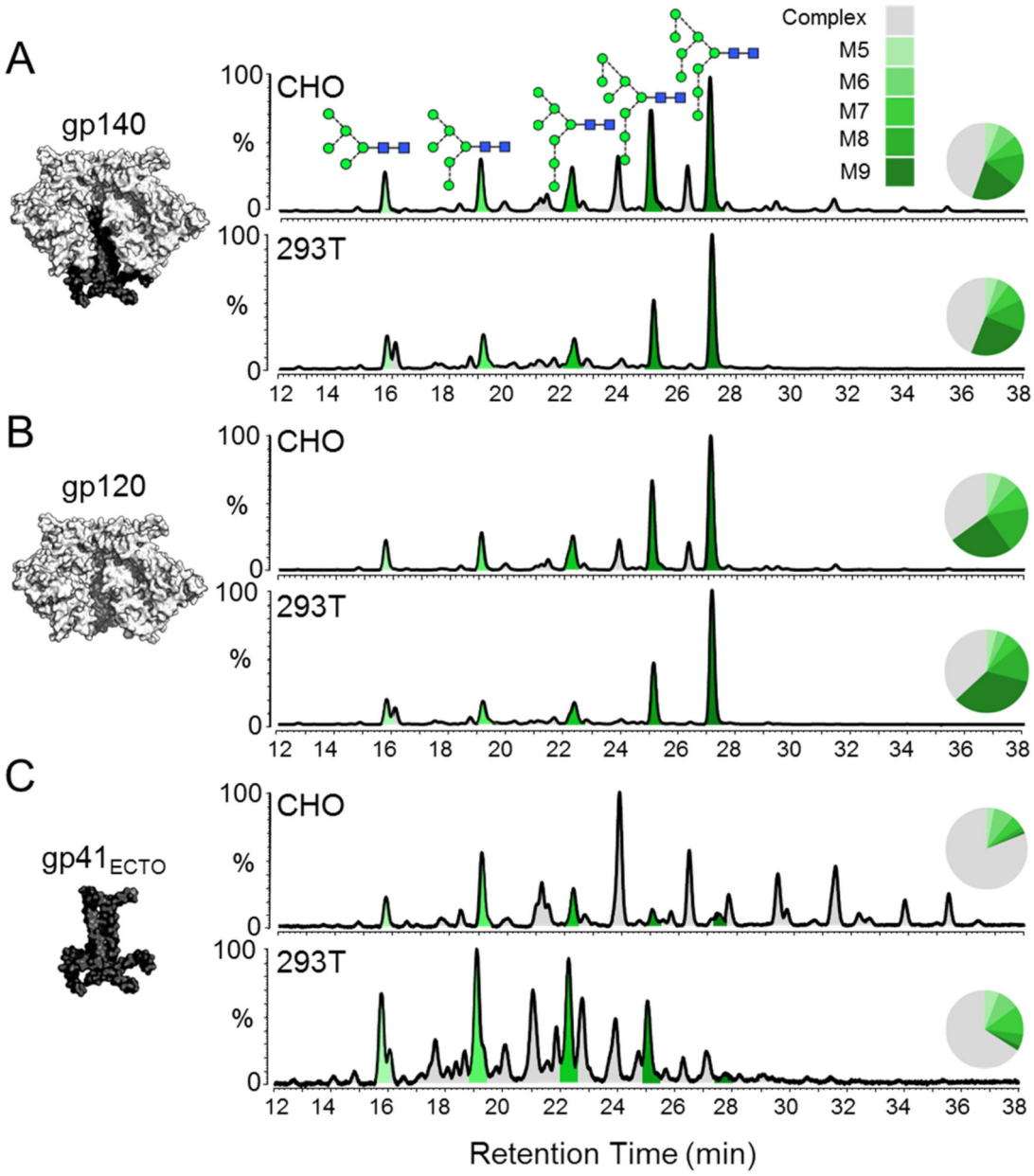

Figure 1. Comparison of glycosylation patterns of BG505 SOSIP.664 trimers produced in CHO and 293T cells

HILIC-UPLC spectra of fluorescently labelled N-linked glycans isolated from (A) the entire trimeric gp120/gp41$_{ECTO}$ complex (gp140), and the (B) gp120 and (C) gp41$_{ECTO}$ subunits of BG505 SOSIP.664 trimers. The subunits analyzed in each case are illustrated on the left. Trimers were purified by 2G12-affinity chromatography followed by SEC. The gp140 band was extracted from a non-reducing SDS-PAGE gel, while the gp120 and gp41$_{ECTO}$ bands were resolved by SDS-PAGE under reducing conditions. The glycan contents of proteins extracted from the bands were analyzed. Peaks corresponding to oligomannose glycans (M5-M9; $Man_{5-9}GlcNAc_2$) are colored in shades of green; the remaining peaks (gray) correspond to complex and hybrid-type glycans. Peak areas (as a % of total glycans) are illustrated in the associated pie charts. Glycan structures are represented according to the

color scheme established by the Consortium for Functional Glycomics (http://www.functionalglycomics.org/). The SOSIP.664 construct contains the following mutations: a T332N mutation to introduce the 332 glycosylation site; cysteines at 501 and 605 form a disulphide bridge to covalently link the gp120 and $gp41_{ECTO}$ subunits; replacement of the gp120 furin cleavage site (RXXR) with a hexa-arginine (R6) sequence to promote furin cleavage; an I559P mutation to stabilize the $gp41_{ECTO}$ subunits in the pre-fusion form; and deletion of the MPER region at residue 664 to reduce aggregation.

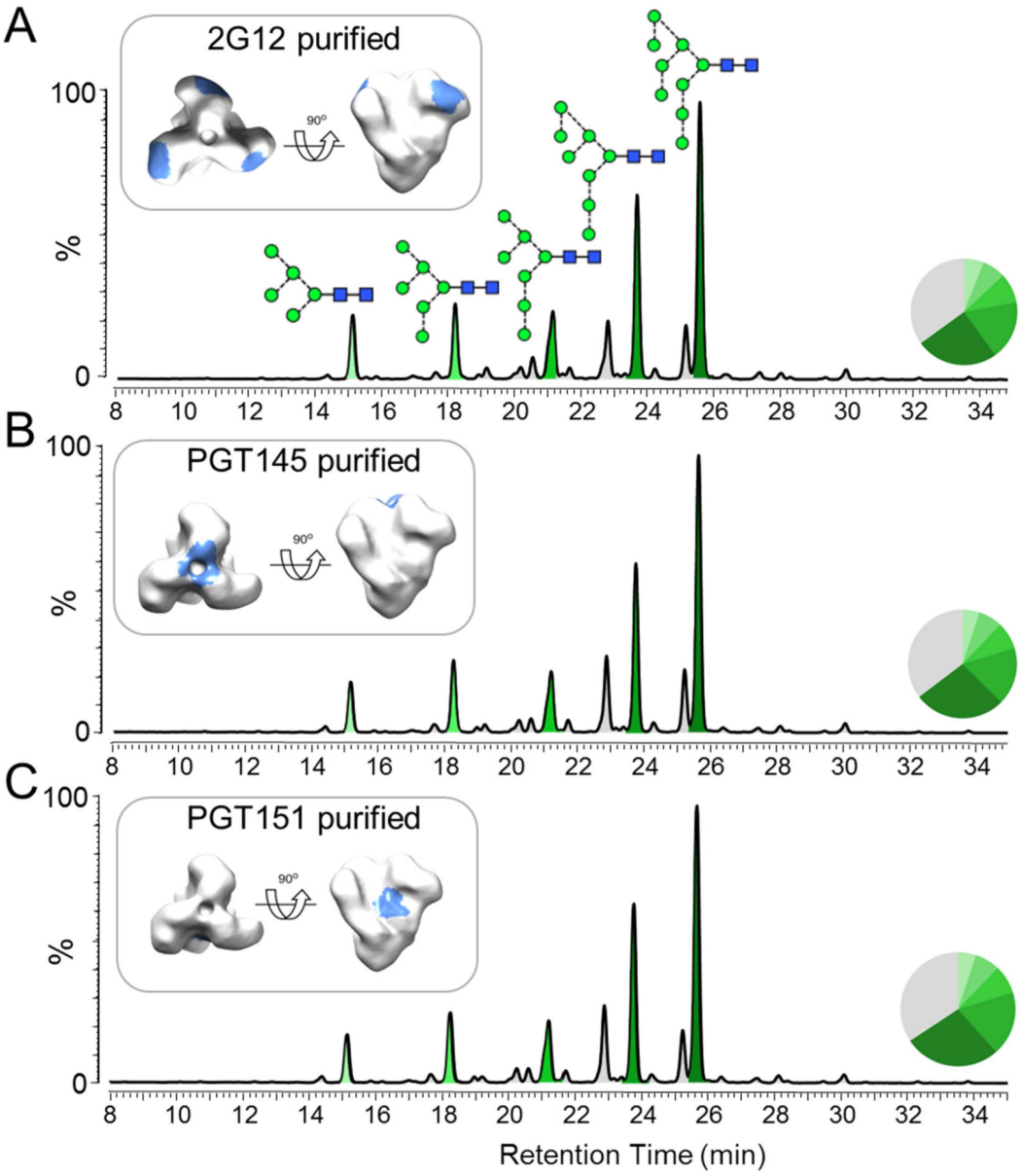

Figure 2. Glycan profiles of BG505 SOSIP.664 trimers following bNAb affinity purification

CHO cell-derived trimers were purified by bNAb affinity chromatography using 2G12, PGT145 or PGT151, followed by SEC. Glycans isolated from reducing SDS-PAGE gels bands containing cleaved gp120 subunits were analyzed by HILIC-UPLC. The various bNAb epitopes are colored light blue on an EM reconstruction on the left. Peaks corresponding to oligomannose glycans are colored in shades of green and the corresponding peak areas are illustrated in the associated pie charts, as in Figure 1.See also Figure S3.

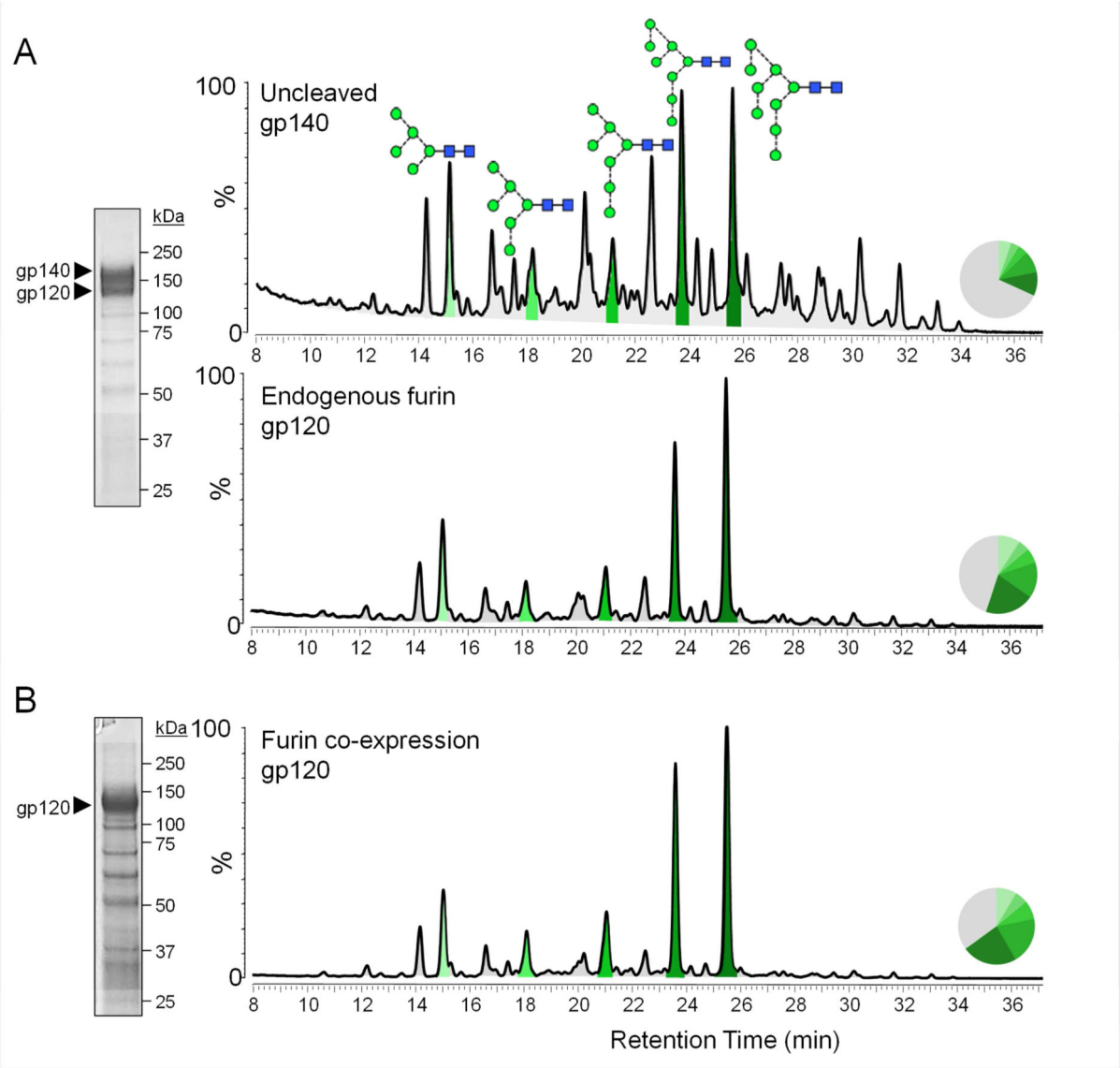

Figure 3. Effect of proteolytic cleavage on Env glycan processing

His-tagged BG505 SOSIP.664 trimers were expressed in 293F cells with and without Furin co-expression and purified by Ni^{2+}-NTA affinity chromatography. (A) Reducing SDS-PAGE of trimers expressed without furin, and the resulting HILIC-UPLC glycan profiles derived from gel bands corresponding to uncleaved gp140 (top panel) and cleaved gp120 (bottom panel). (B)Reducing SDS-PAGE of the same trimers but co-expressed with Furin, and the corresponding HILIC-UPLC glycan profiles derived from the band corresponding to cleaved gp120. Peaks corresponding to oligomannose glycans are colored in shades of green and the corresponding peak areas are illustrated in the associated pie charts, as in Figure 1. SDS-PAGE analysis in both panels reveals a minor population of low molecular weight contaminants.

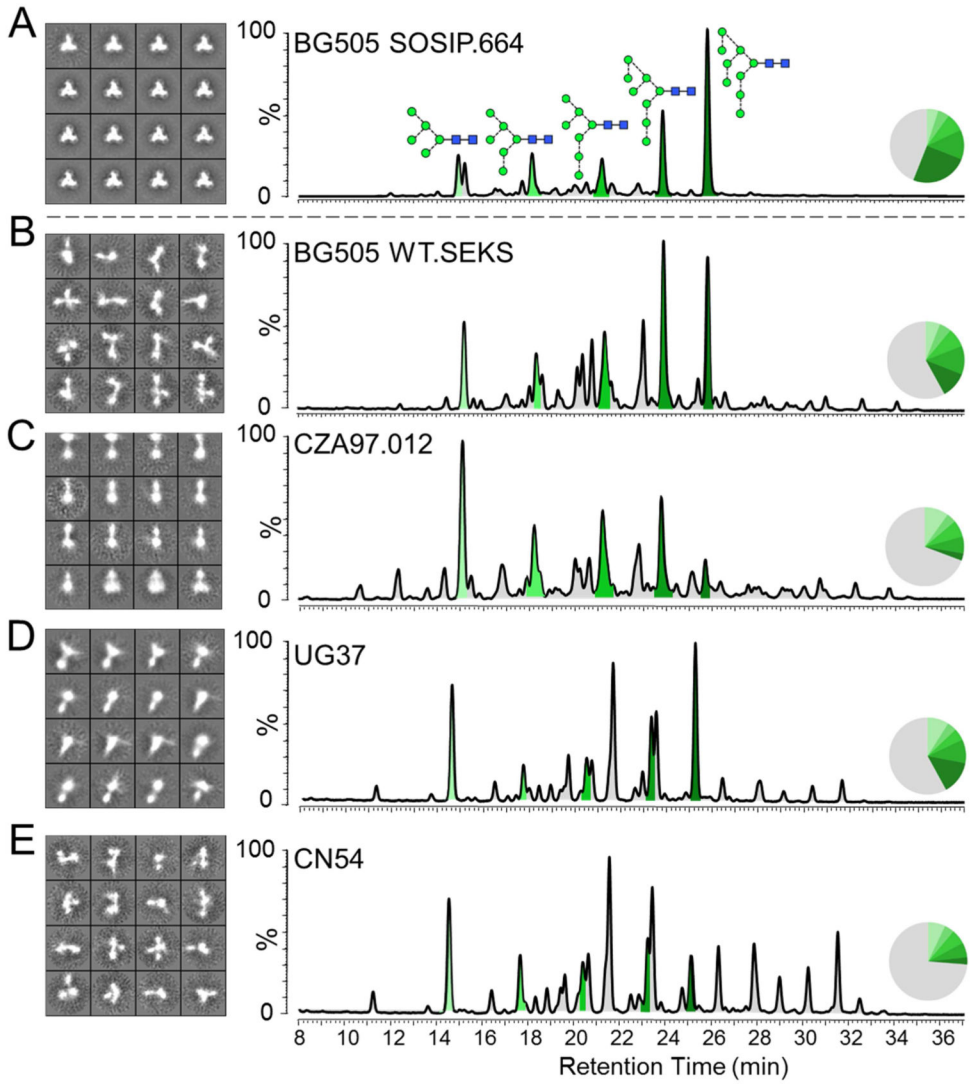

Figure 4. Disordered configurations of uncleaved gp140s are associated with higher levels of glycan processing

HILIC-UPLC glycan data and 2D class averages from negative stain EM analysis are shown for: (A) BG505 SOSIP.664 trimers expressed in 293T cells and purified using 2G12 affinity chromatography followed by SEC. The UPLC chromatogram is reproduced from Figure 1A to facilitate data comparison. (B) Uncleaved BG505 WT.SEKS gp140 expressed in 293T cells and purified by 2G12 affinity chromatography followed by SEC. Quantitation of the complete datasets show that native-like, regular and compact trimers constitute >90% of the images of the BG505 SOSIP.664 proteins. In contrast, <5% of the uncleaved BG505 WT.SEKS proteins are in native-like form, where the predominant images represent

disordered, splayed out trimers. The same is also true of: (C) uncleaved, His-tagged CZA97.012 gp140 proteins produced in 293T cells and purified by Ni^{2+}-NTA affinity chromatography followed by SEC; (D) uncleaved UG37 gp140; (E) uncleaved CN54 gp140 proteins (the latter two purchased from Polymun Scientific, Vienna, Austria). Peaks corresponding to oligomannose glycans are colored in shades of green and the corresponding peak areas are illustrated in the associated pie charts, as in Figure 1.

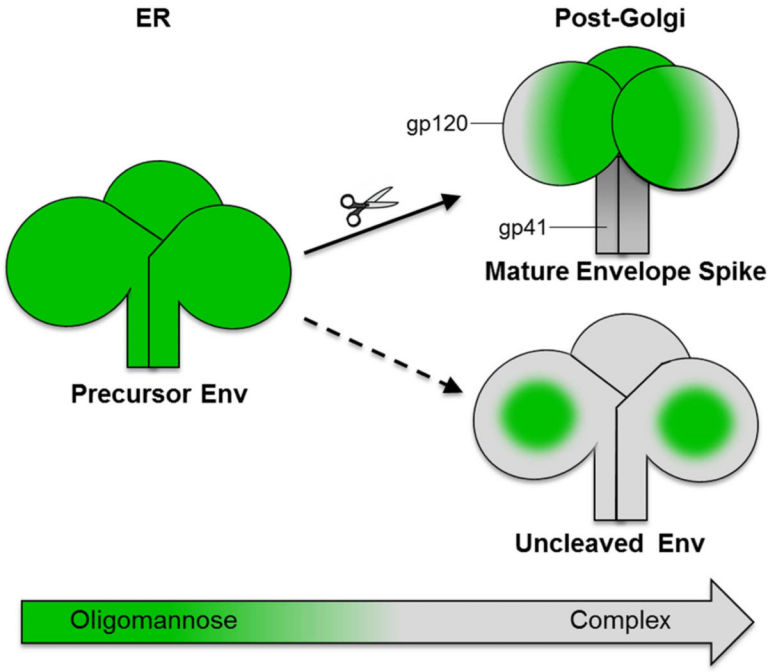

Figure 5. Env cleavage induces highly homogenous glycoforms dominated by oligomannose glycans

Env is synthesized as a gp160 precursor in the ER and oligomannose-type glycans are incorporated at glycosylation sequons: Asn-Ser/Thr-X (where X is any amino acid except Pro). As glycoproteins pass through the secretory pathway they are exposed to α-mannosidases and other glycan processing enzymes, which normally convert oligomannose-type glycans (green) to complex-type glycans (gray). The quaternary structure of Env dictates how well processing enzymes can access the glycans on gp120. Cleaved Env exhibits a compact quaternary structure that prevents trimming by ER and Golgi α-mannosidases, and is thus secreted as an oligomannose-dominated glycoform. In contrast, uncleaved Env has a more open and irregular structure that facilitates easier access by processing enzymes, leading to conversion of the majority of the oligomannose glycans to more complex-type structures. However, high glycan density on the outer domain of gp120 creates a region that is largely protected from α-mannosidase trimming, known as the intrinsic mannose patch, which is present on both cleaved and uncleaved Env. Gp41 is more accessible to processing enzymes than gp120 and is dominated by complex-type glycosylation.

Table 1

Abundances of oligomannose glycans in different Env proteins

Env protein	Producer cell	Affinity purification scheme	Abundance (% of total glycans)					
			M‡	M6	M7	M8	M9	Total
gp120$_{BG505}$ from cleaved trimers								
SOSIP.664	CHO	PGT151	5	7	8	18	27	**66**
SOSIP.664	CHO	PGT145	5	7	8	17	27	**65**
SOSIP.664	CHO	2G12	6	7	9	18	25	**65**
SOSIP.664	293T	2G12	4	4	6	15	34	**63**
SOSIP.664	293F	2G12	8	5	8	19	20	**60**
SOSIP.664	293F	PGT151	9	5	8	24	25	**71**
gp41ECTO$_{BG505}$ from cleaved trimers								
SOSIP.664	CHO	2G12	3	8	5	2	1	**19**
SOSIP.664	293T	2G12	6	9	12	5	2	**34**
gp140 from cleaved[a] and uncleaved[b] trimers§								
SOSIP.664[a]	CHO	2G12	6	8	8	14	20	**55**
SOSIP.664[a]	293T	2G12	5	5	8	13	25	**56**
BG505 WT.SEKS[b]	293T	2G12	6	5	8	12	11	**42**
CZA97.012[b]	293T	Ni^{2+}-NTA	10	4	7	7	3	**30**
CN54gp140[b]	CHO	5F3	7	4	6	6	3	**27**
UG37gp140[b]	CHO	5F3	9	4	5	10	14	**42**

‡Mx refers to $Man_xGlcNAc_2$ glycans.

§Glycan profiles for gp140 constructs include contributions from both gp120 and gp41$_{ECTO}$ domains.